Electronic Supplementary Material (ESI) for Chemical Communications

Supplementary Information

Lithium Cation Enhances Anion Binding in a Tripodal Phosphine Oxide-Based Ditopic Receptor

Jesse V. Gavette,[a] Juven Lara,[a] Orion B. Berryman,[a] Lev N. Zakharov,[a] Michael M. Haley[a]* and Darren W. Johnson[a]*

[a] Department of Chemistry and the Materials Science Institute, University of Oregon, Eugene, OR 97403-1253

E-mail: dwj@uoregon.edu; haley@uoregon.edu

Table of Contents

1. Synthesis and Characterization

1.1 General Methods and Details

Tetrabutylammonium salts were dried at 50 °C under vacuum and stored in a calcium carbonate filled dessicator. All other materials were obtained from TCI-America, Sigma-Aldrich, or Acros and used as received. Reactions were performed under an inert N_2 atmosphere in dried glassware. ^{1}H, ^{13}C and ^{31}P nuclear magnetic resonance spectra were recorded using an Agilent VNMRS 600 (^{1}H: 600.0 MHz; ^{13}C: 150.9 MHz; ^{31}P: 242.9 MHz), a Varian Inova 500 (^{1}H: 500.1 MHz; ^{13}C: 121.4 MHz; ^{31}P: 202.3 MHz) and a Varian Inova 300 (^{1}H: 299.9 MHz) and are reported as parts per million (ppm) downfield shift of tetramethylsilane (δ_H 0.00), in deuterochloroform ($CDCl_3$, δ_H 7.26 ppm), deuterodimethylsulfoxide (DMSO-d_6, δ_H 2.50 ppm; δ_C 39.52 ppm), deuteroacetonitrile (MeCN-d_3, δ_H 1.94 ppm) or deuteromethanol (CD_3OD, δ_C 49.00 ppm) as internal references, and ^{31}P nuclear magnetic resonance spectra are reported as parts per million (ppm) shifted of 1% H_3PO_4 (δ_P 0.00 ppm) in deuterium oxide (D_2O) as an external reference, unless otherwise stated.[1,2] The data is reported as chemical shift (δ), multiplicity (br = broad, s = singlet, d = doublet, t = triplet, q = quartet, m = multiplet), coupling constant (*J* Hz) and relative integral. Atmospheric pressure chemical ionization spectra were recorded using an Agilent 1100 Series LC/MSD.

1.2 Experimental Details

Ditopic Receptor (2). N-(tert-Butoxycarbonyl)glycine (0.505 g, 2.88 mmol) was added to DMF (6 mL) and cooled to 0°C. HBTU (1.22 g, 3.21 mmol) and DIPEA (0.56 mL) were added and the mixture stirred under N_2 for 15 min. Trihydrobromide salt **1a** (0.351 g, 0.925 mmol) and DIPEA

(1.23 mL) were added to the mixture. The reaction was stirred overnight under N_2 at room temperature. The solvent was removed and the resulting yellow residue was taken up in hot EtOAc. Upon cooling a white precipitate formed which was isolated to afford **2** as an analytically pure white powder (0.426 g, 76%); m.p. 110-115 °C. ^{1}H NMR (300 MHz, DMSO-d_6) δ 8.19 (t, J = 5.8 Hz, 3H), 7.11 (t, J = 5.6 Hz, 3H), 3.60-3.55 (m, 12H), 1.37 (s, 27H); ^{13}C NMR (126 MHz, DMSO-d_6) δ 170.16, 155.89, 78.22, 43.40, 28.17; ^{13}C NMR (150.9 MHz, CD_3OD) δ 173.29, 158.50, 80.87, 44.88, 36.59 (d, J_{PC} = 68.5 Hz), 28.73; ^{31}P NMR (121 MHz, DMSO-d_6) δ 41.11; M.S (APCI+) m/z = 609.2 $[M+H]^+$.

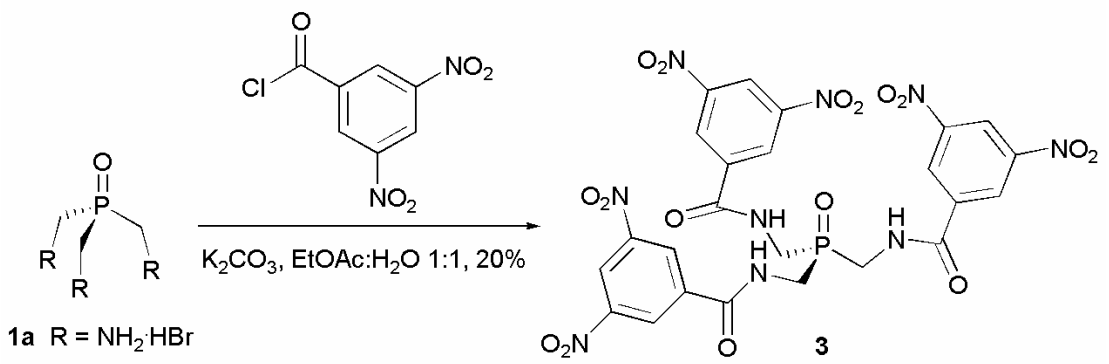

Scheme S1. Synthesis of receptor **3**.

Receptor (3)[3]**.** Trihydrobromide salt **1a** (0.406g, 1.07 mmol) and K_2CO_3 (0.915g, 6.62 mmol) were dissolved in a mixture of EtOAc:H_2O 1:1 (120 mL). To this solution was added 3,5-dinitrobenzoyl chloride (0.840g, 3.64 mmol) in EtOAc (8 mL) dropwise with vigorous stirring. After stiring vigorously for 23 h, the organic layer was isolated and the solvent was removed via a stream of air. The crude solid was washed with EtOH resulting in a white powder (0.152 g, 20%); m.p. 166 °C (decomp); ^{1}H NMR (600 MHz, DMSO-d_6) δ 9.76 (t, J = 5.9 Hz, 2H), 9.08 (d, J = 2.1 Hz, 3H), 8.98 (t, J = 2.0 Hz, 2H), 4.15 (t, J = 5.7 Hz, 4H); ^{13}C NMR (150.9 MHz, DMSO-d_6) δ 162.82, 148.13, 136.22, 127.67, 121.07, 37.91 (d, J_{PC} = 65.5 Hz); ^{31}P NMR (242.9 MHz, DMSO-d_6) δ 40.93.

2. ^{1}H, ^{13}C and ^{31}P NMR Spectra

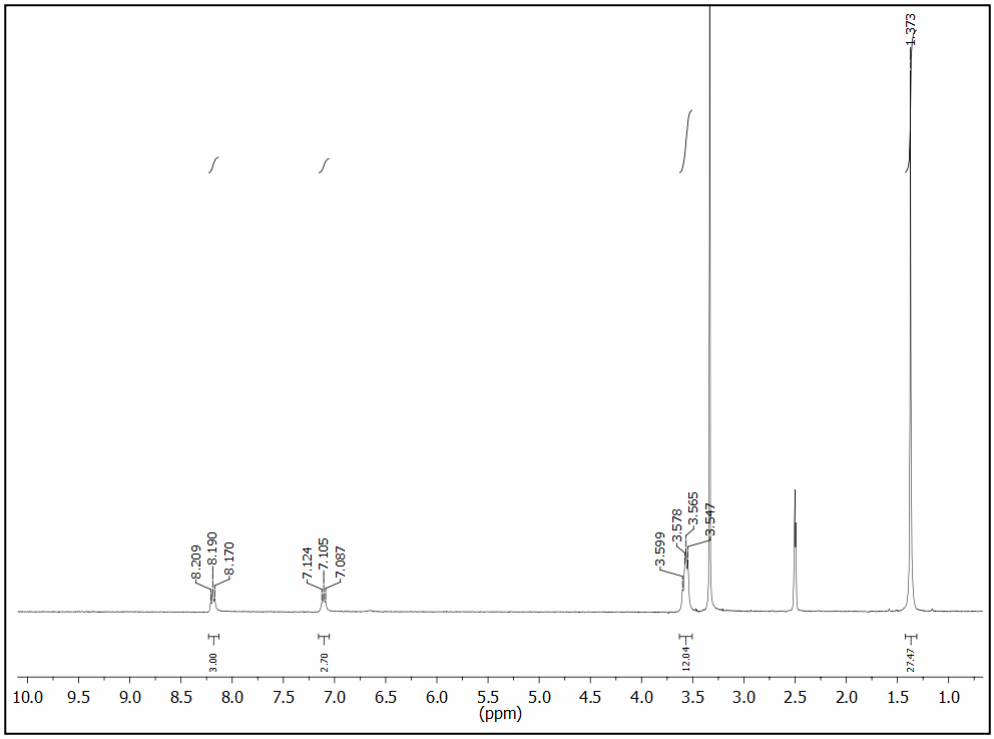

Fig. S1. ^{1}H NMR spectrum of **2**, 300 MHz, DMSO-d_6.

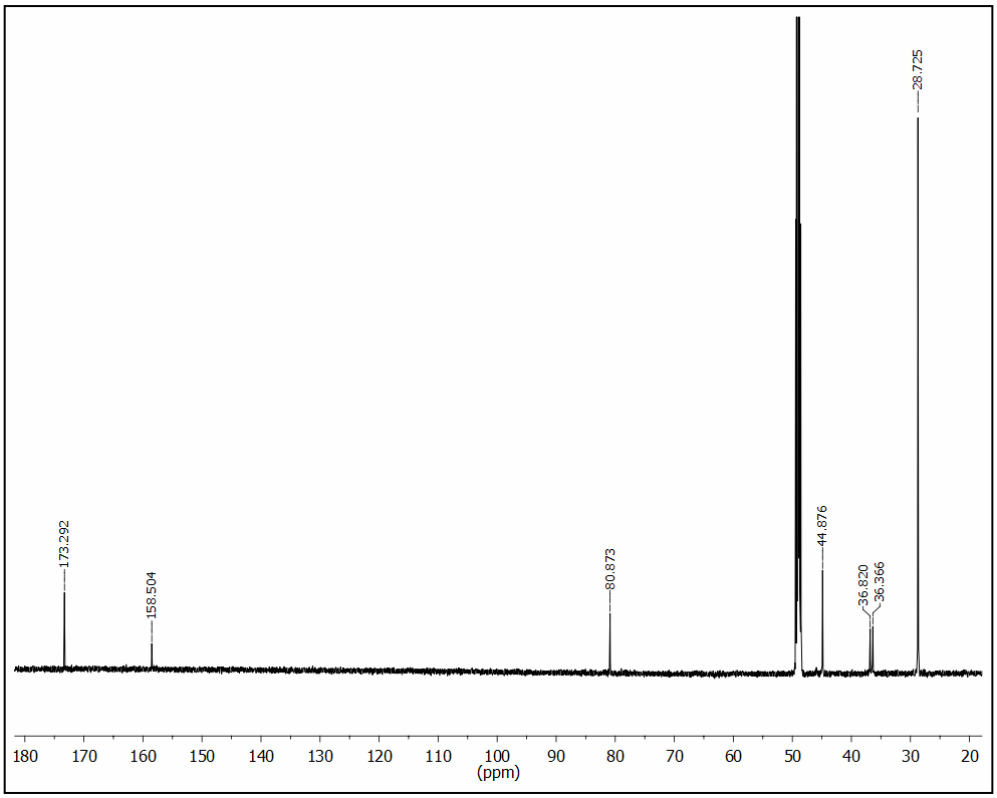

Fig. S2. ^{13}C NMR spectrum of **2**, 151 MHz, CD_3OD.

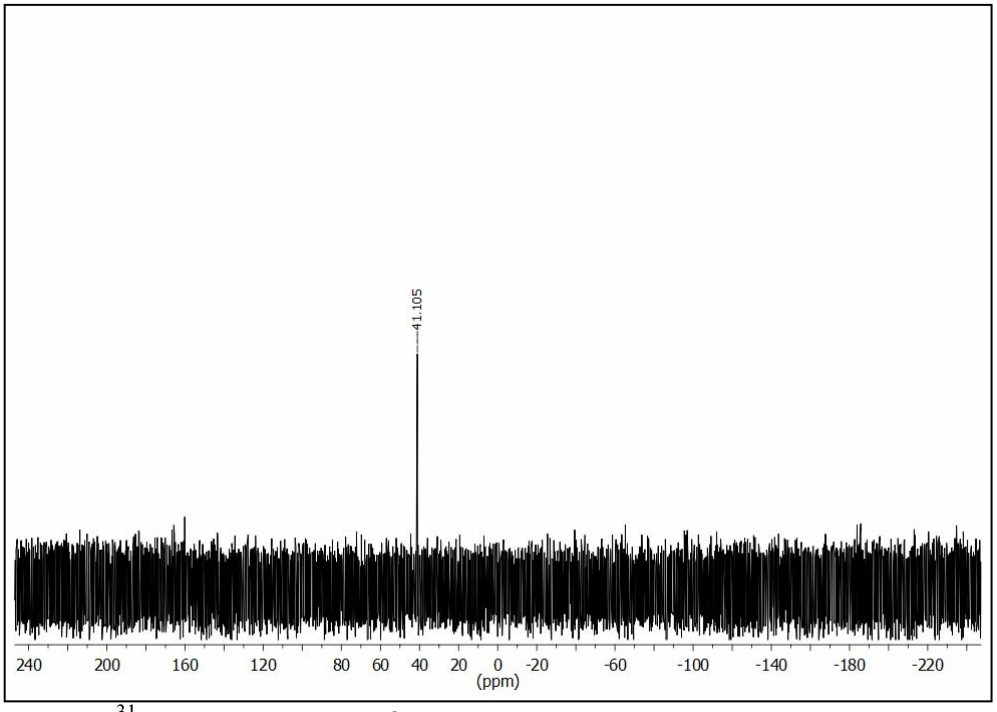

Fig. S3. ^{31}P NMR spectrum of **2**, 202 MHz, DMSO-d_6.

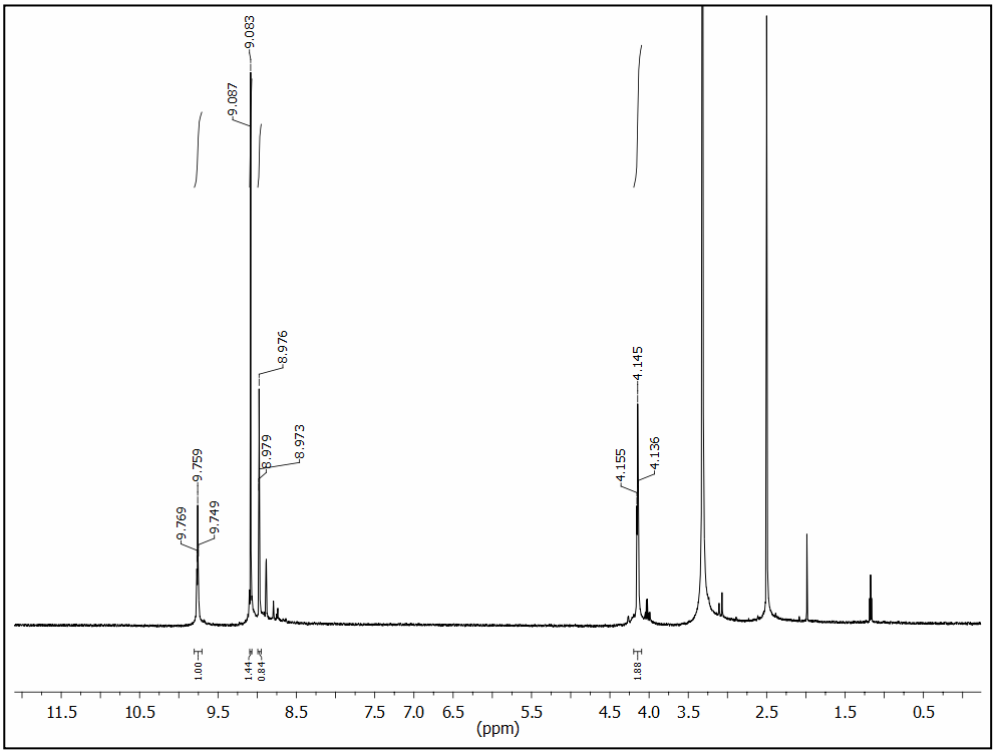

Fig. S4. ^{1}H NMR spectrum of **3**, 600 MHz, DMSO-d_6.

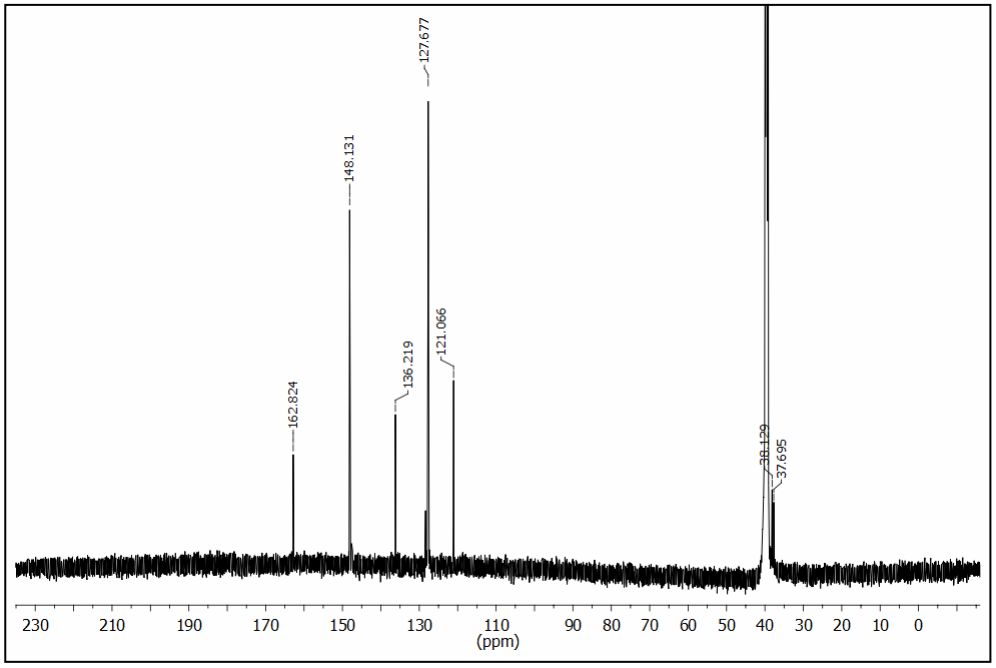

Fig. S5. ^{13}C NMR spectrum of **3**, 151 MHz, DMSO-d_6.

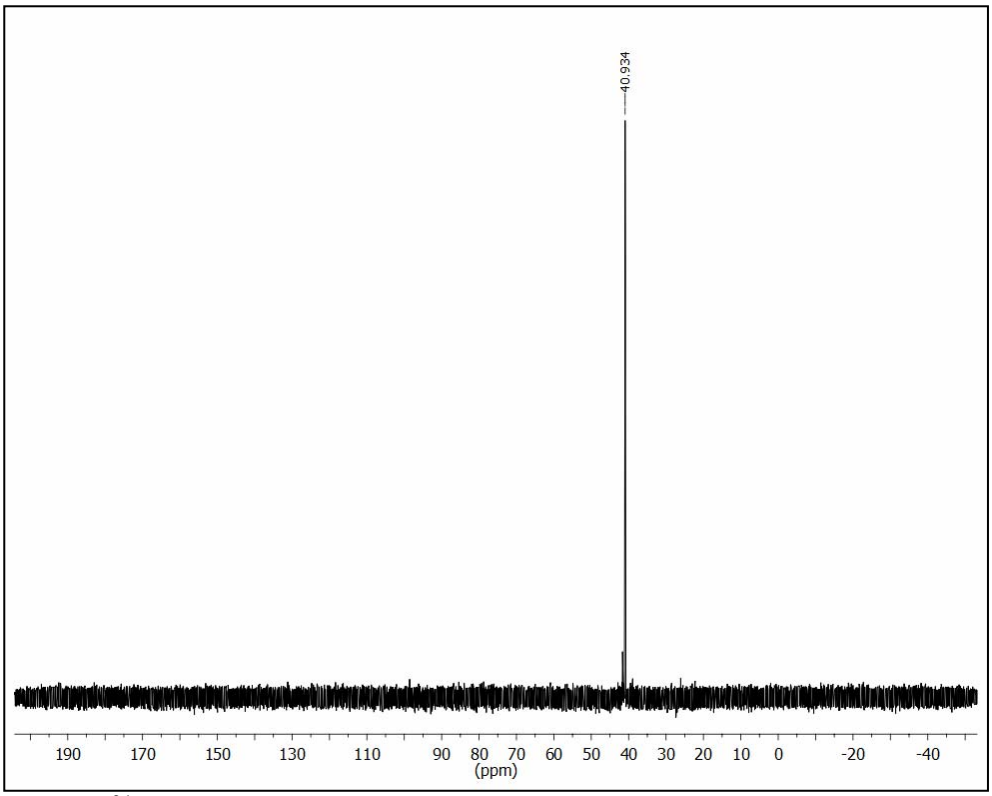

Fig. S6. ^{31}P NMR spectrum of **3**, 243 MHz, DMSO-d_6.

3. Job's Plots for Complexes of 2[4]

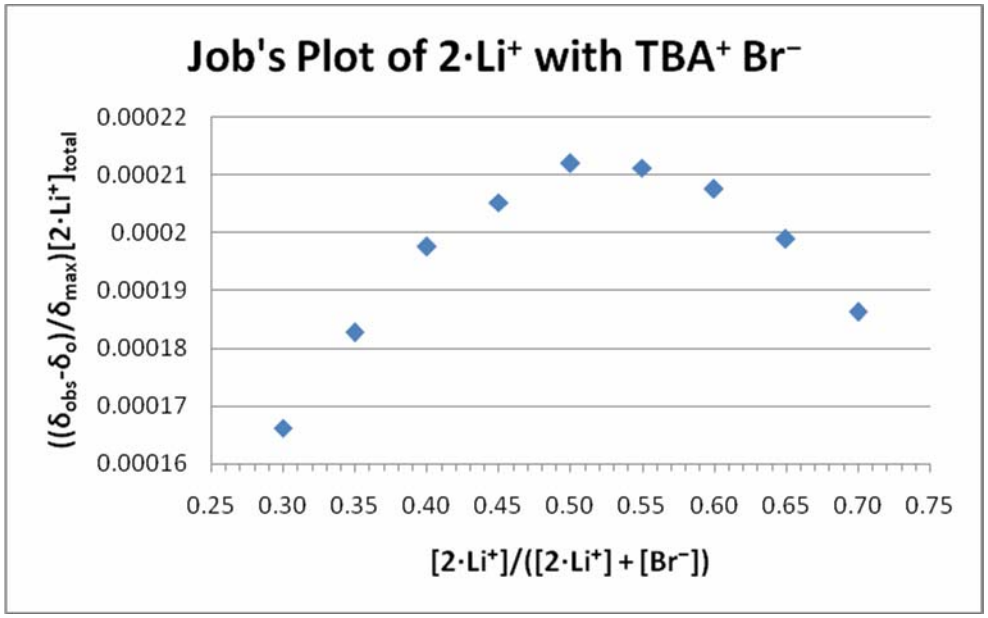

Fig. S7. Job plot for the mixture of **2**·Li^+ and Br^- (MeCN-d_3), [Li^+] = 0.0100 M, [**2**] + [Br^-] = 0.0020 M.

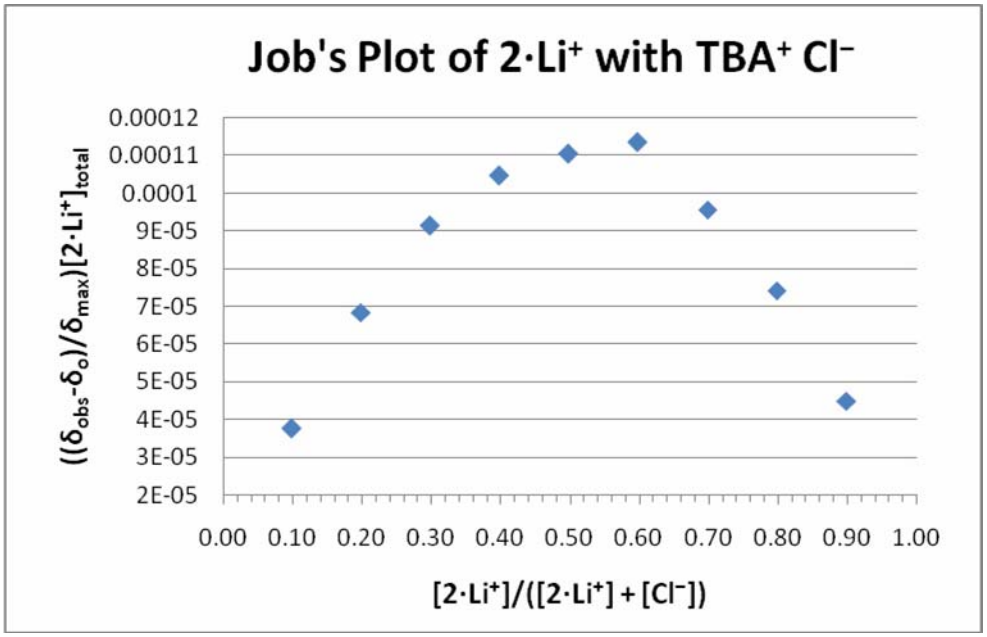

Fig. S8. Job plot for the mixture of **2**·Li^+ and Cl^- (MeCN-d_3), [Li^+] = 0.0051 M, [**2**] + [Cl^-] = 0.0010 M.

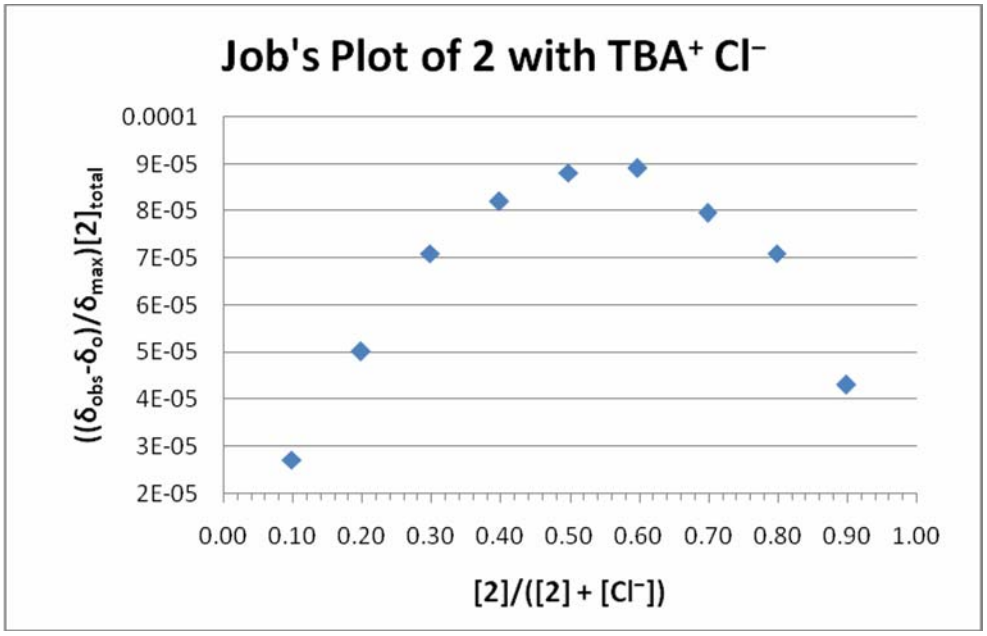

Fig. S9. Job plot for the mixture of **2** and Cl^- (MeCN-d_3), [**2**] + [Cl^-] = 0.0010 M.

4. Binding Studies for 2, 2·Li^+ and 2·Na^+

4.1 General Notes for titration experiments

A 5 mM stock solution of **2** was prepared using MeCN-d_3 in a volumetric flask. Aliquots of stock solutions of **2** were diluted with the same solvent in a separate volumetric flask to yield a solution of approximately 0.0005 M concentration. In each case, 500 μL of this solution was transferred to an NMR tube, and the remainder of the solution was used to make the guest stock solution to a concentration of 0.010 – 0.080 M to maintain a constant host concentration throughout the titration. Aliquots of the guest solution were added via Hamilton gas tight syringes to the host solution in the NMR tube, and a spectrum was obtain via either a Varian Inova 500 or an Agilent VNMRS 600 spectrometer at 298 K after thorough mixing. Association constants (K_a) were calculated by non-linear curve fitting of the obtained titration isotherms using WinEQNMR2.[5] The reported association constants were calculated from the downfield shifting of the carbamate proton resonance. All titrations were performed in triplicate.

4.2 Titrations of 2

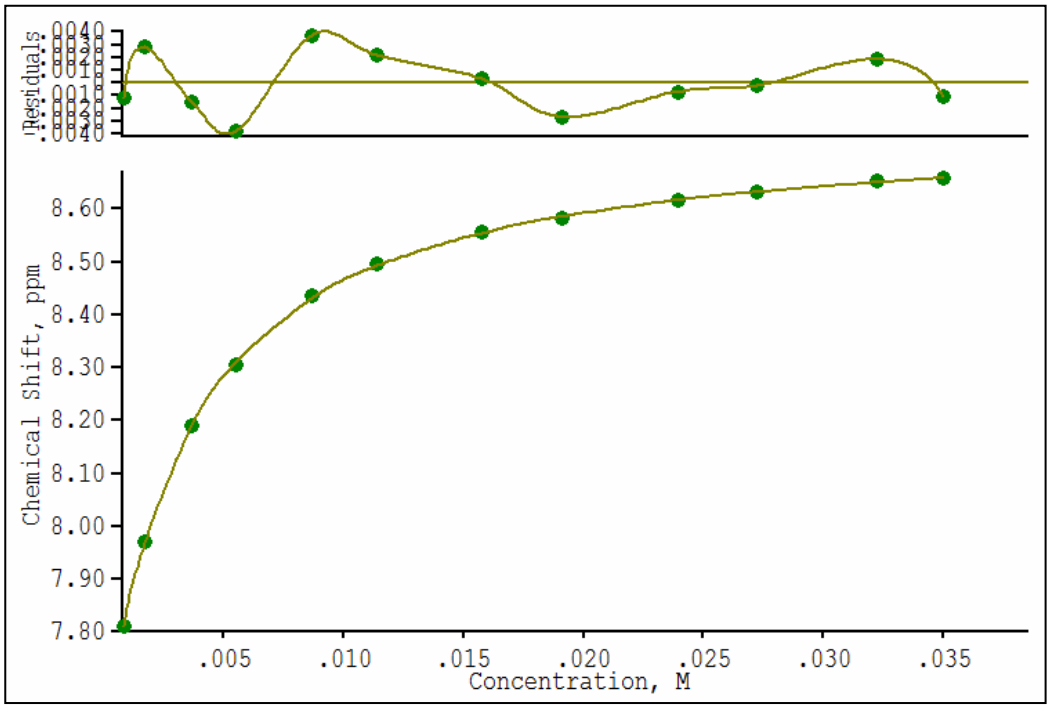

Fig. S10. Binding curve from ^{1}H NMR titration of **2** with TBA^{+} Cl^{-} in MeCN-d_3, δ_{Host} (ppm) vs. [Cl^{-}] M.

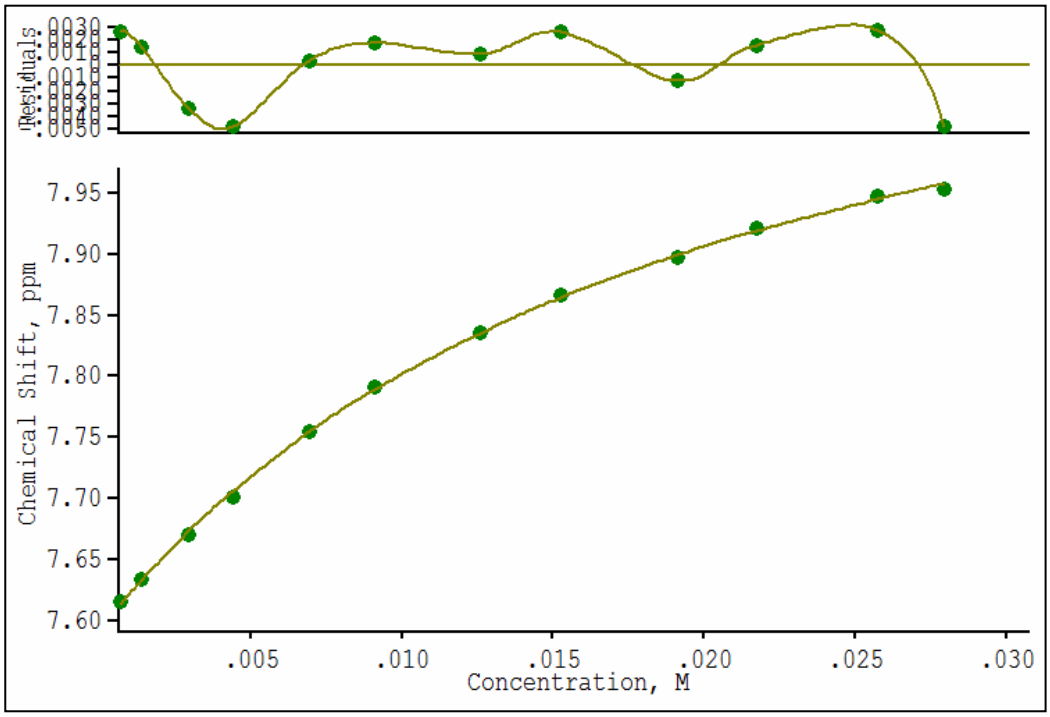

Fig. S11. Binding curve from ^{1}H NMR titration of **2** with TBA^{+} Br^{-} in MeCN-d_3, δ_{Host} (ppm) vs. [Br^{-}] M.

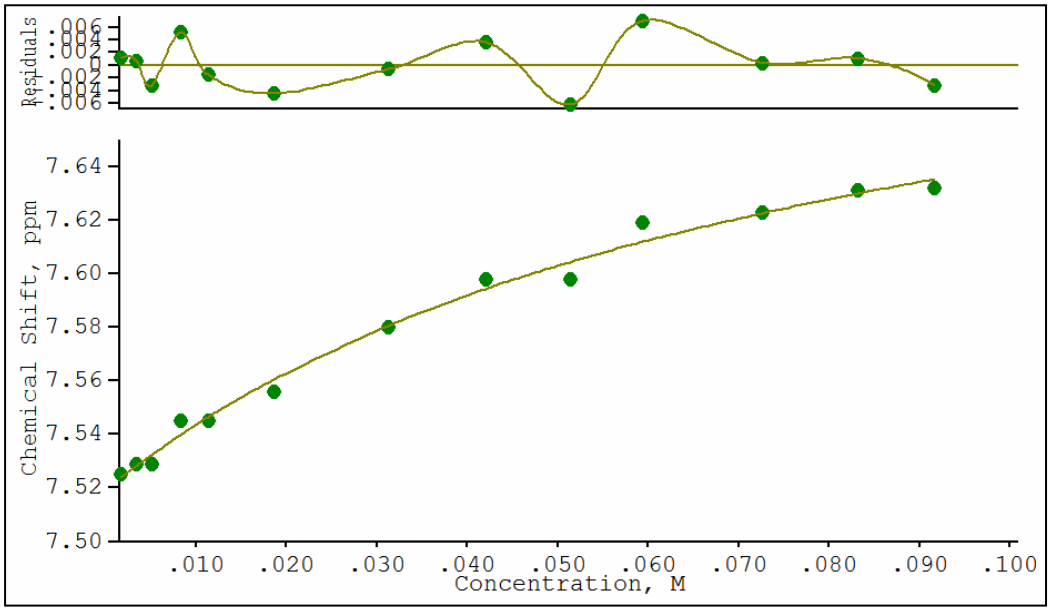

Fig. S12. Binding curve from ^{1}H NMR titration of **2** with $TBA^+ I^-$ in MeCN-d_3, δ_{Host} (ppm) vs. [I^-] M.

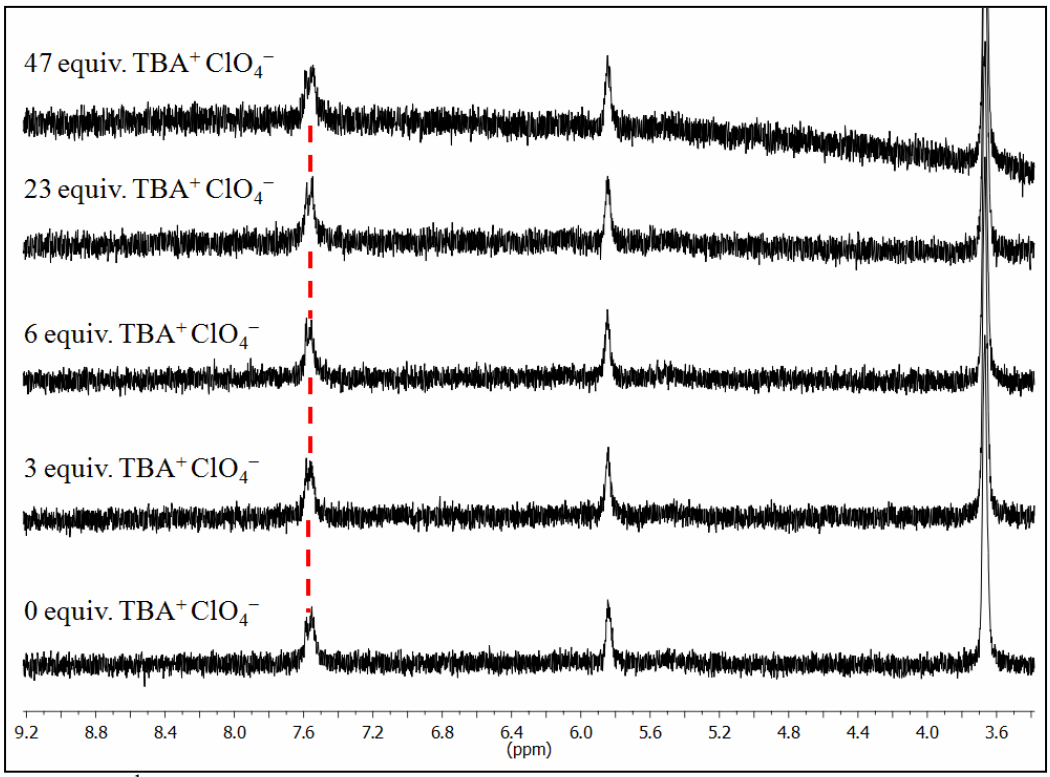

Fig. S13. ^{1}H NMR spectra of **2** with varying amounts of TBA perchlorate.

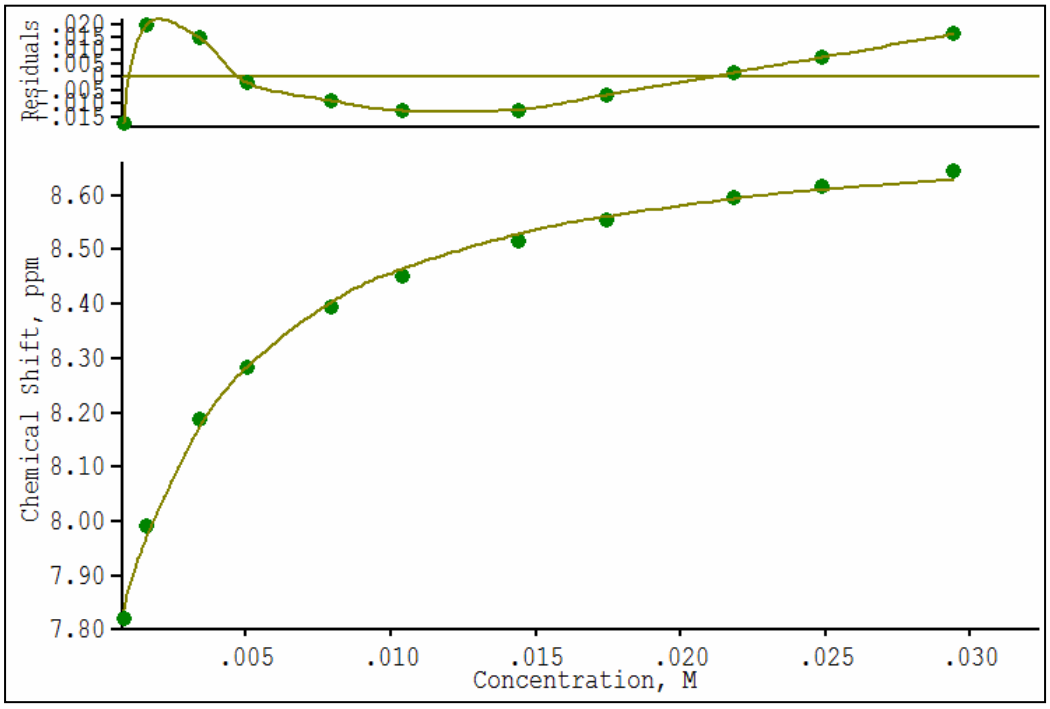

Fig. S14. Binding curve from ^{1}H NMR titration of **2** with LiBr in MeCN-d_3, δ_{Host} (ppm) vs. [LiBr] M.

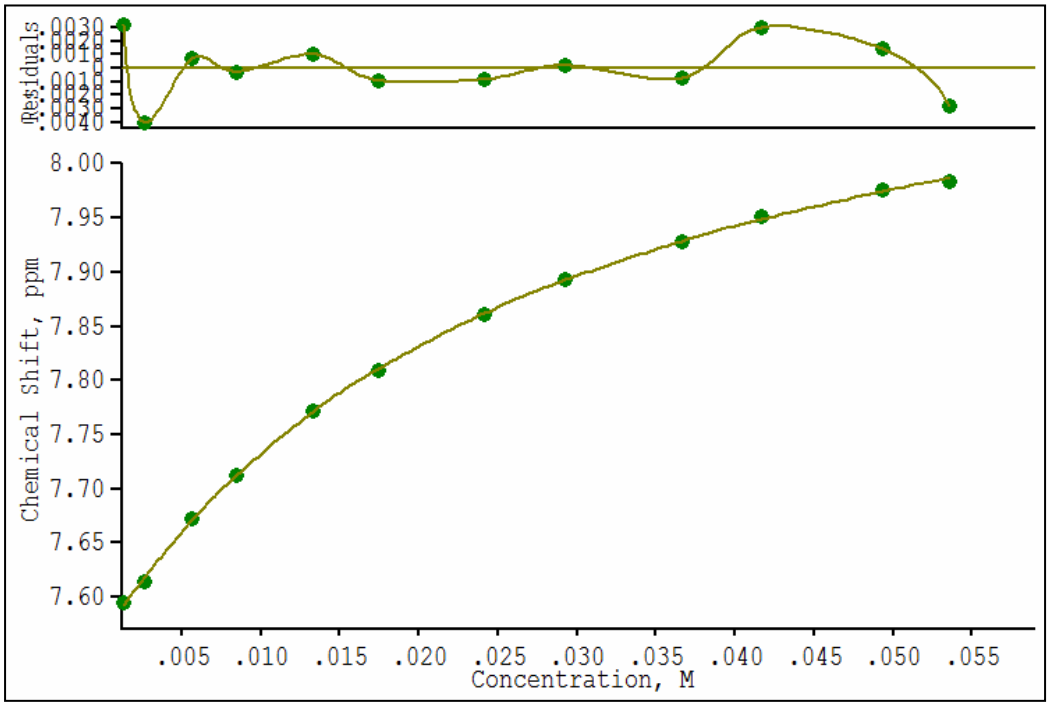

Fig. S15. Binding curve from ^{1}H NMR titration of **2** with LiI in MeCN-d_3, δ_{Host} (ppm) vs. [LiI] M.

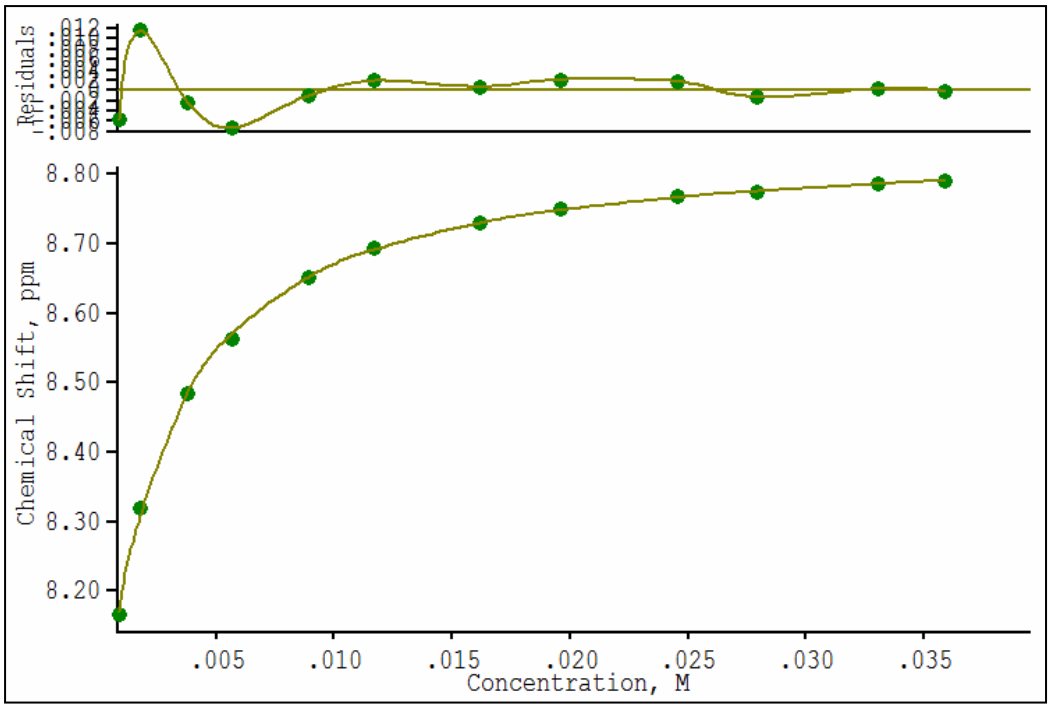

Fig. S16. Binding curve from ^{1}H NMR titration of **2**·Li^{+} with TBA^{+} Cl^{-} in MeCN-d_3, δ_{Host} (ppm) vs. [Cl^{-}] M.

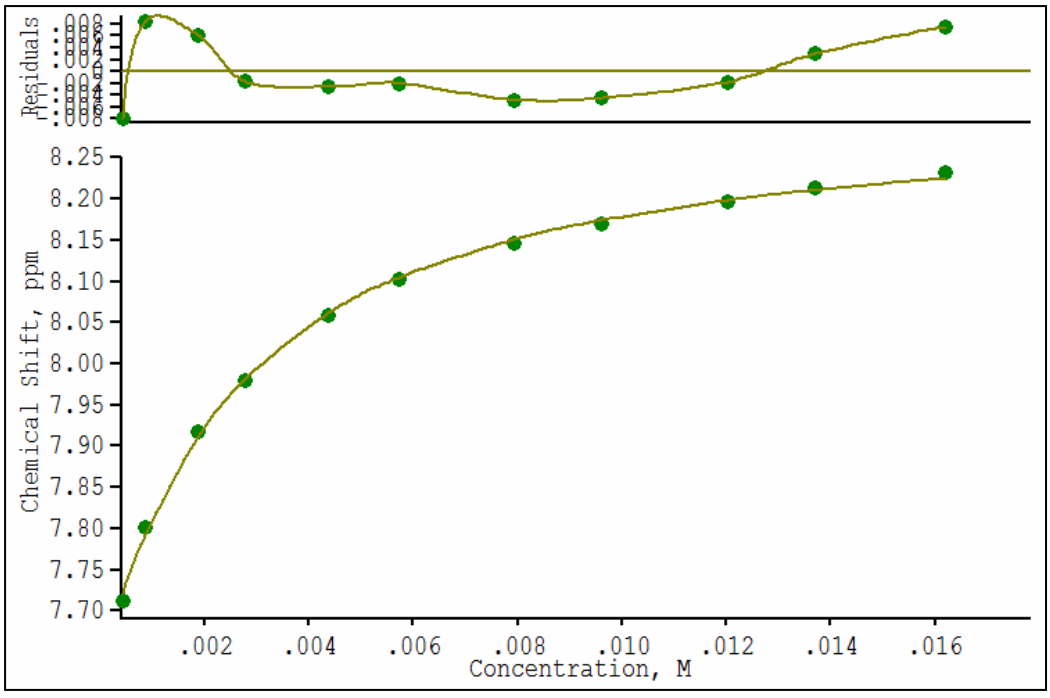

Fig. S17. Binding curve from ^{1}H NMR titration of **2**·Li^{+} with TBA^{+} Br^{-} in MeCN-d_3, δ_{Host} (ppm) vs. [Br^{-}] M.

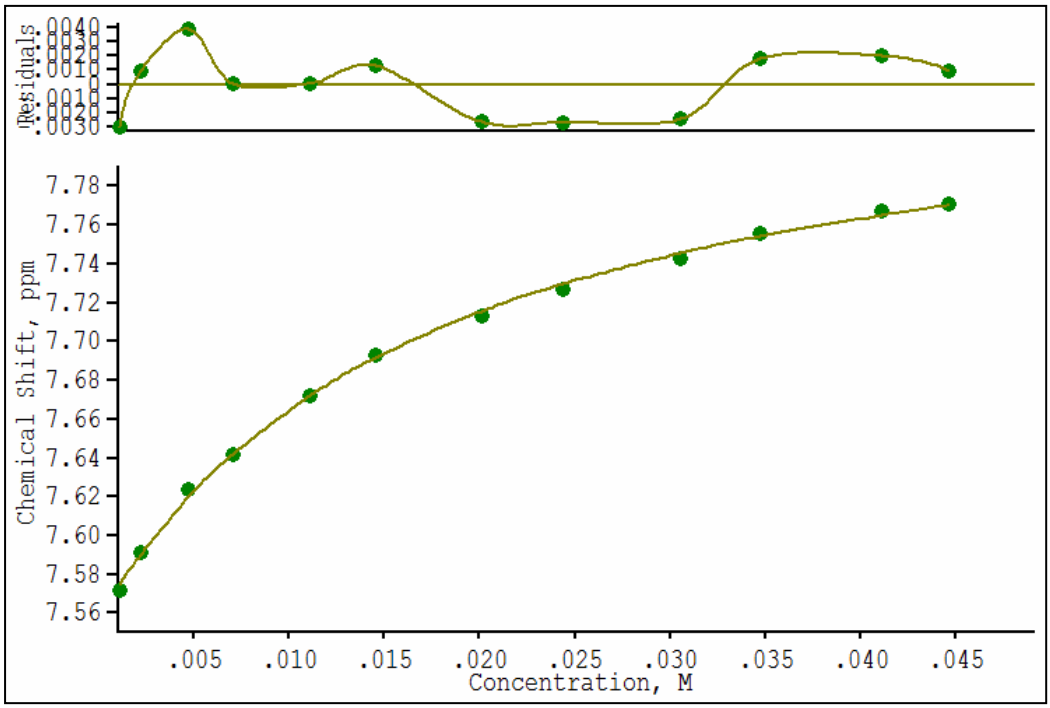

Fig. S18. Binding curve from ^{1}H NMR titration of **2**·Li^{+} with TBA^{+} I^{-} in MeCN-d_3, δ_{Host} (ppm) vs. [I^{-}] M.

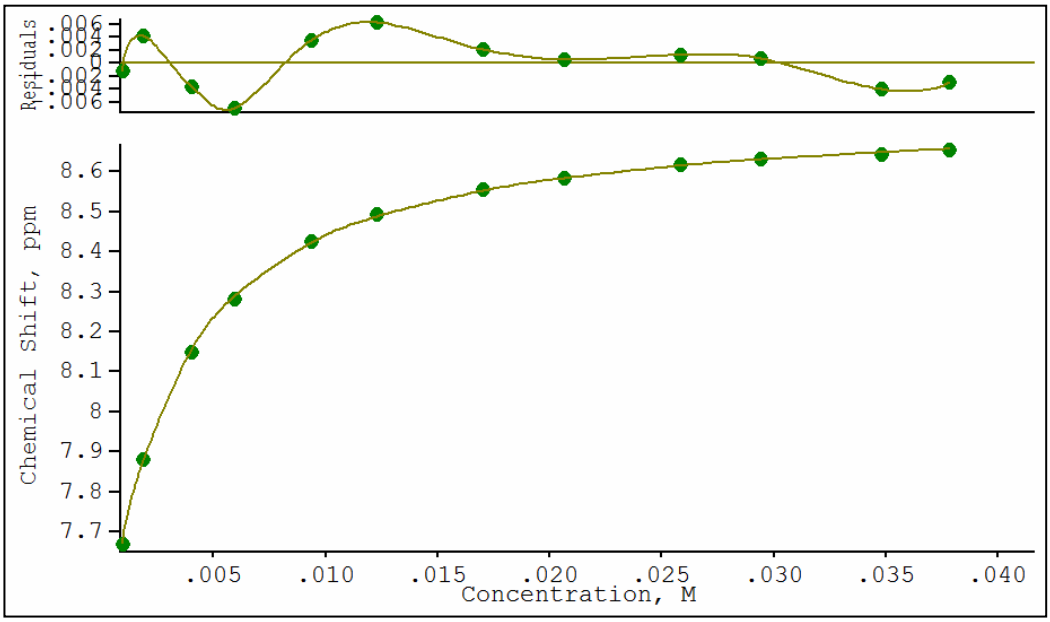

Fig. S19. Binding curve from ^{1}H NMR titration of **2**·Na^{+} with TBA^{+} Cl^{-} in MeCN-d_3, δ_{Host} (ppm) vs. [Cl^{-}] M.

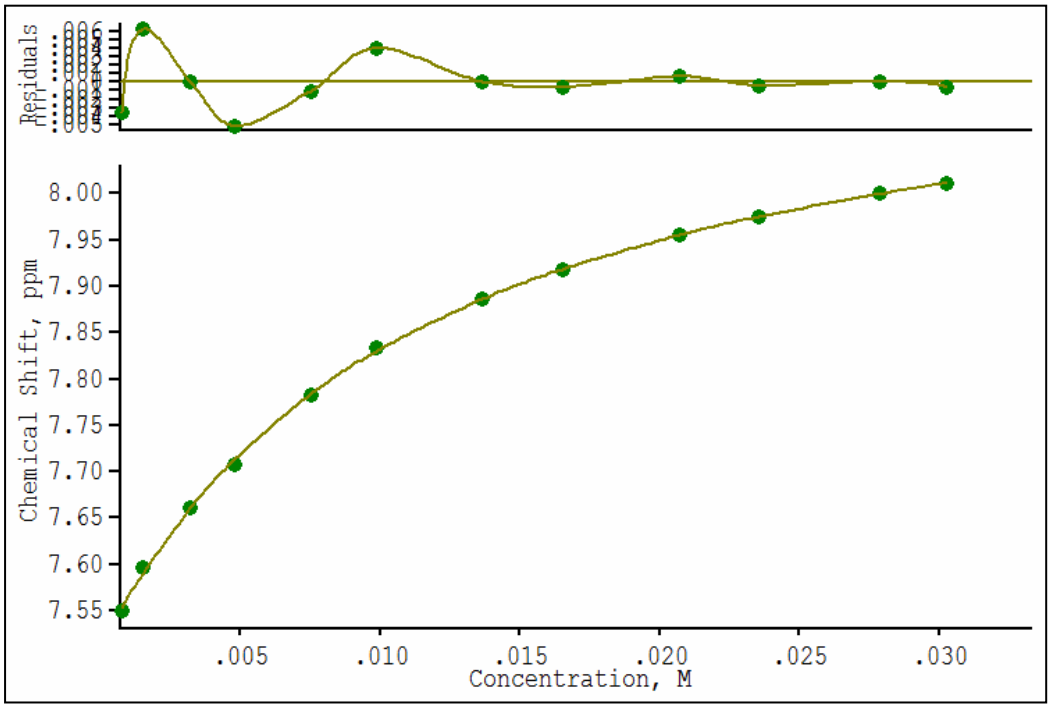

Fig. S20. Binding curve from ^{1}H NMR titration of **2**·Na^{+} with TBA^{+} Br^{-} in MeCN-d_3, δ_{Host} (ppm) vs. [Br^{-}] M.

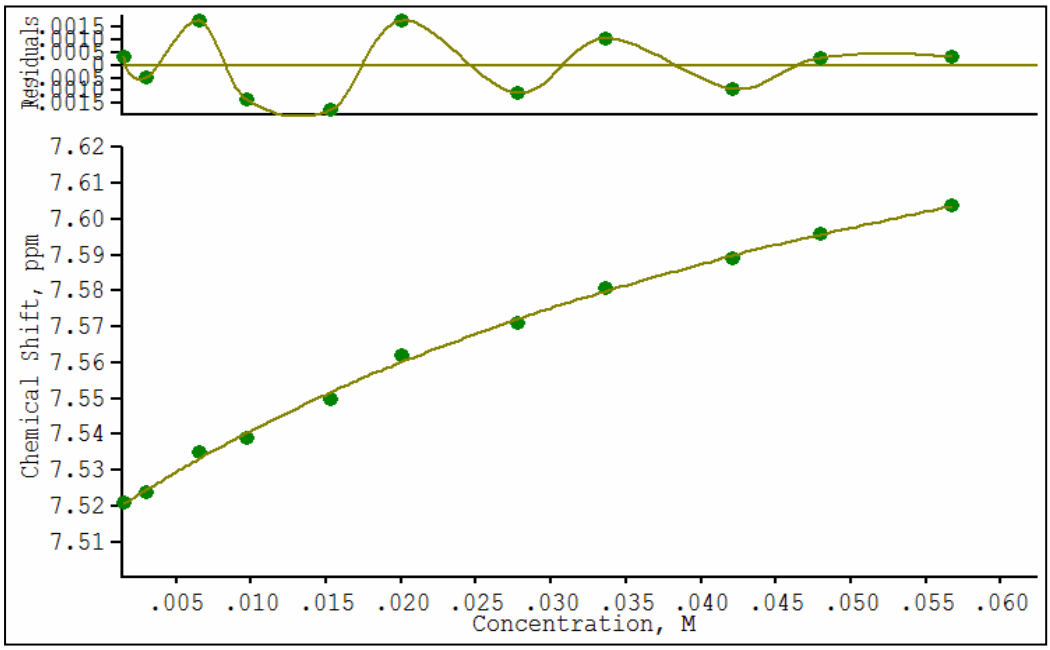

Fig. S21. Binding curve from ^{1}H NMR titration of **2**·Na^{+} with TBA^{+} I^{-} in MeCN-d_3, δ_{Host} (ppm) vs. [I^{-}] M.

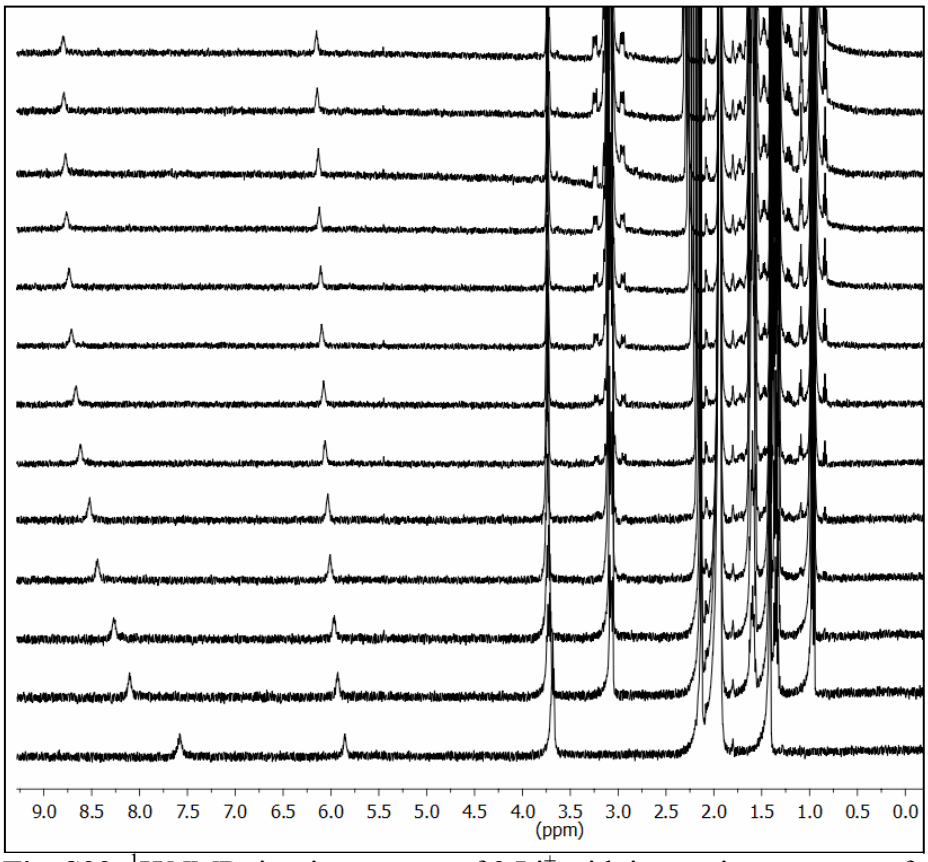

Fig. S22. ^{1}H NMR titration spectra of **2**·Li^{+} with increasing amounts of TBA^{+} Cl^{-} in MeCN-d_3(bottom to top).

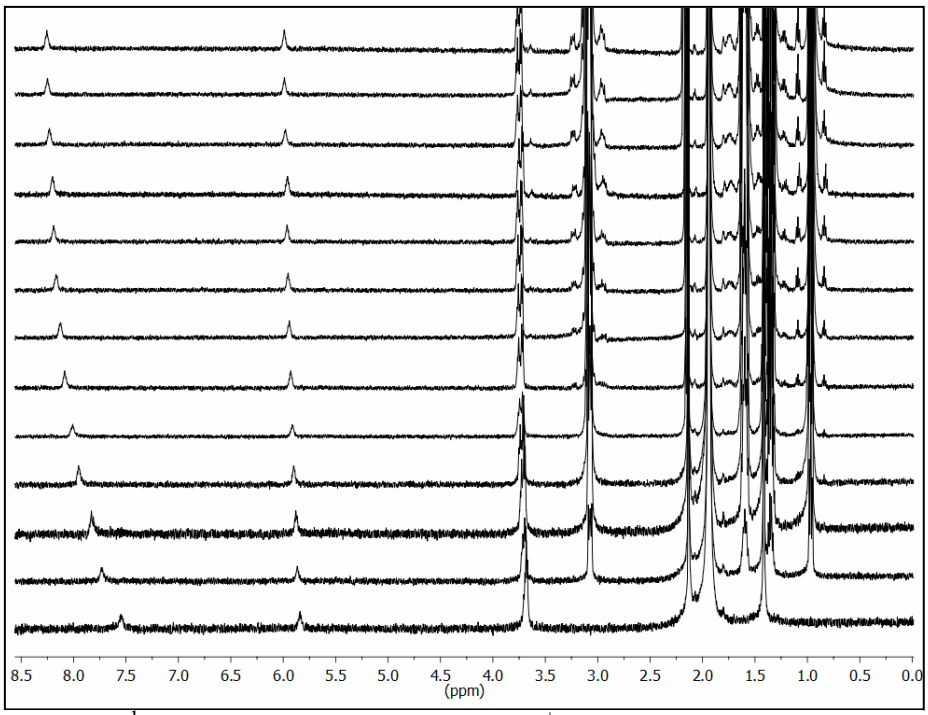

Fig. S23. ^{1}H NMR titration spectra of **2**·Li^{+} with increasing amounts of TBA^{+} Br^{-} in MeCN-d_3(bottom to top).

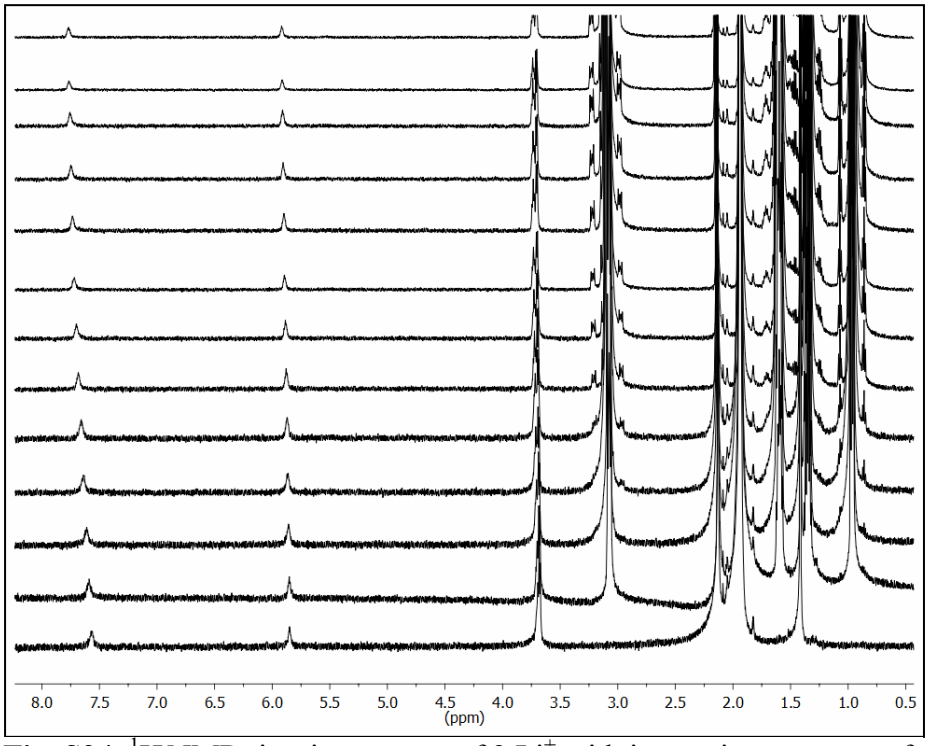

Fig. S24. ^{1}H NMR titration spectra of **2**·Li^{+} with increasing amounts of TBA^{+} I^{-} in MeCN-d_3(bottom to top).

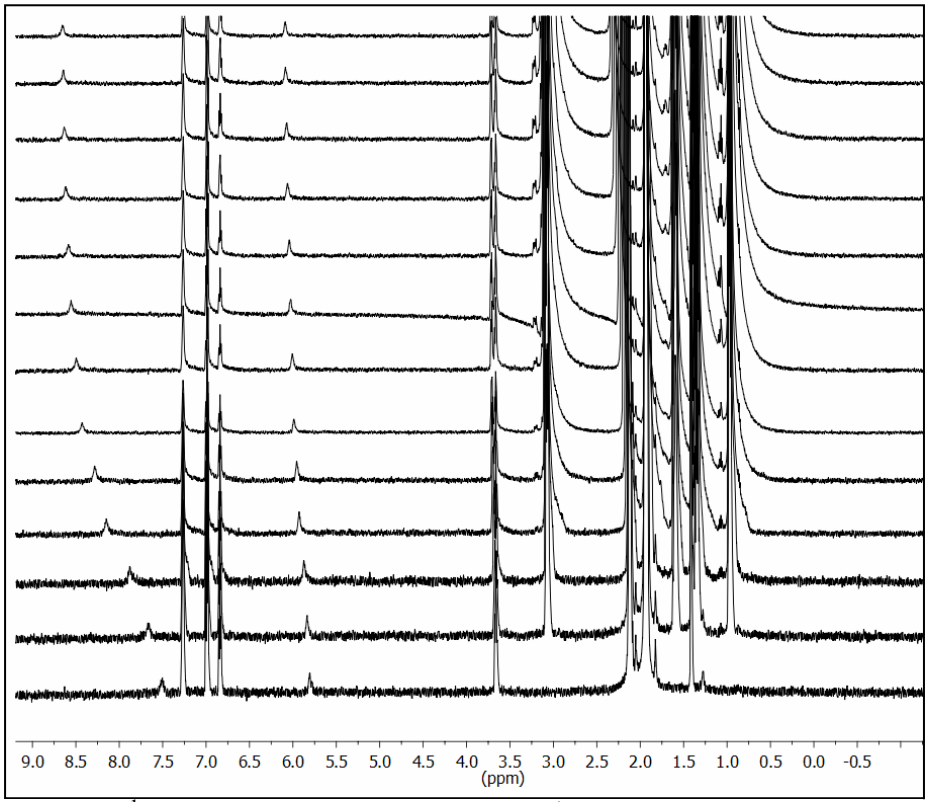

Fig. S25. ^{1}H NMR titration spectra of **2**·Na^{+} with increasing amounts of TBA^{+} Cl^{-} in MeCN-d_3(bottom to top).

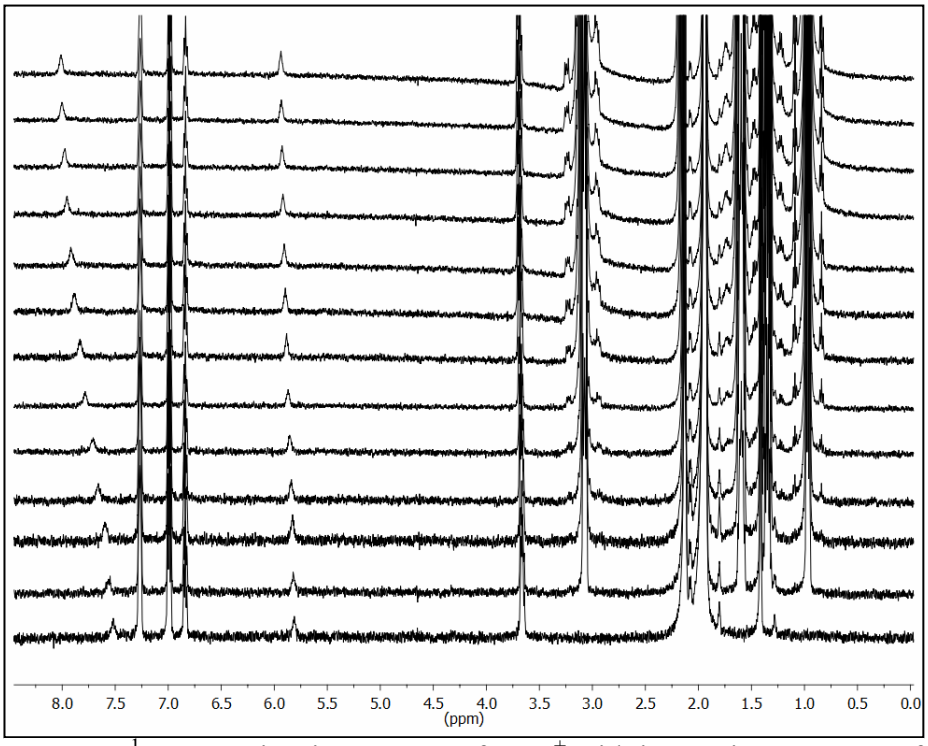

Fig. S26. ^{1}H NMR titration spectra of **2**·Na^{+} with increasing amounts of TBA^{+} Br^{-} in MeCN-d_3(bottom to top).

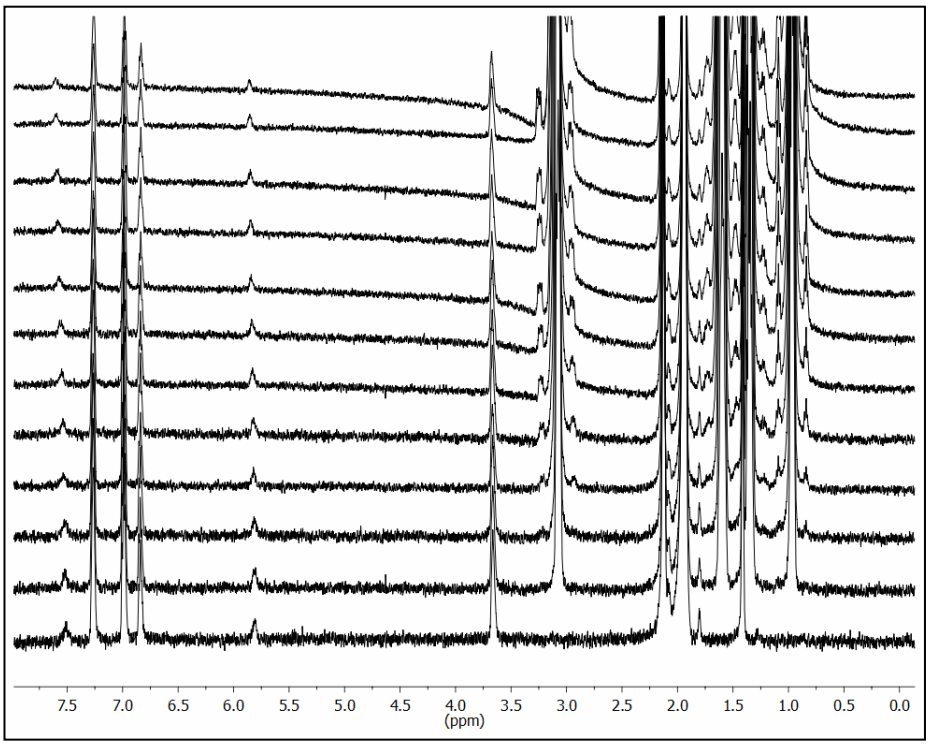

Fig. S27. ^{1}H NMR titration spectra of **2**·Na^{+} with increasing amounts of TBA^{+} I^{-} in MeCN-d_3(bottom to top).

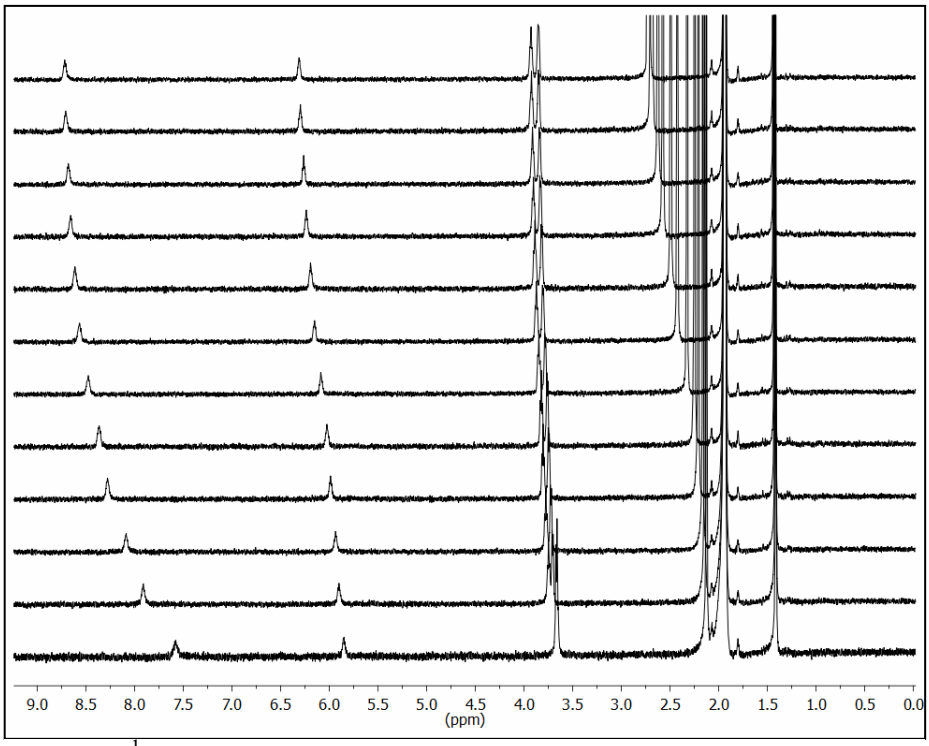

Fig. S28. ^{1}H NMR titration spectra of **2** with increasing amounts of LiBr in MeCN-d_3(bottom to top).

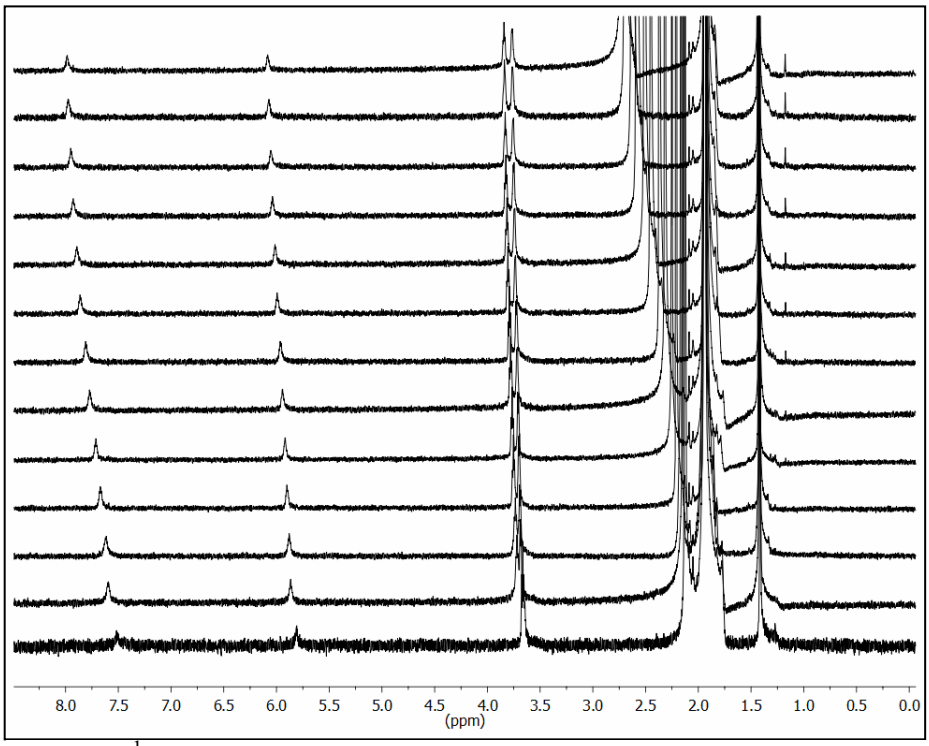

Fig. S29. ^{1}H NMR titration spectra of **2** with increasing amounts of LiI in MeCN-d_3(bottom to top).

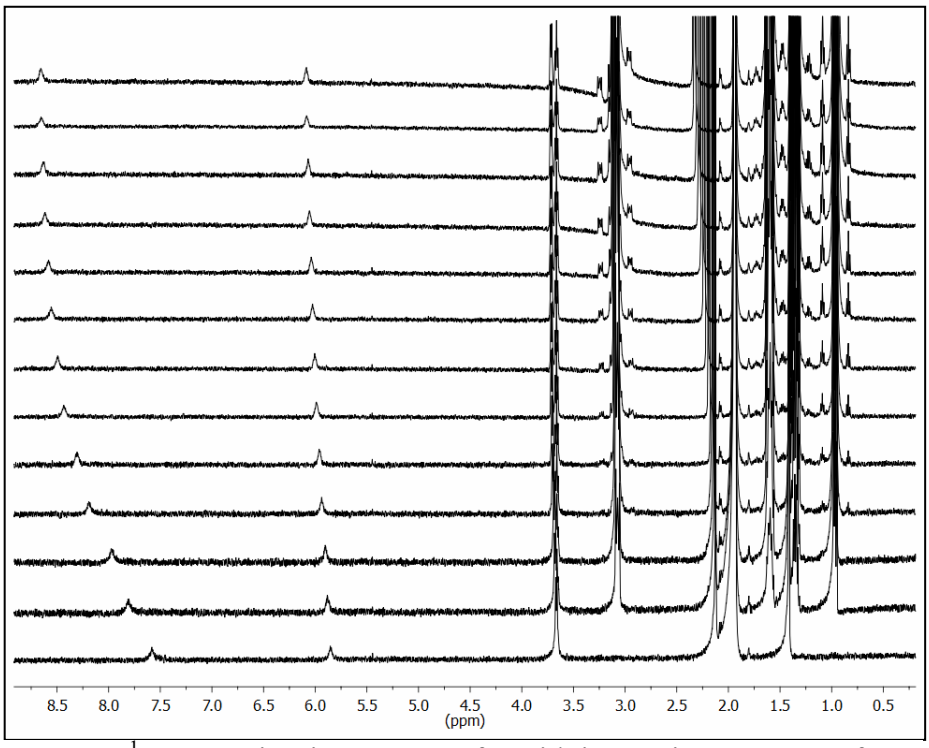

Fig. S30. ^{1}H NMR titration spectra of **2** with increasing amounts of TBA^{+} Cl^{-} in MeCN-d_3(bottom to top).

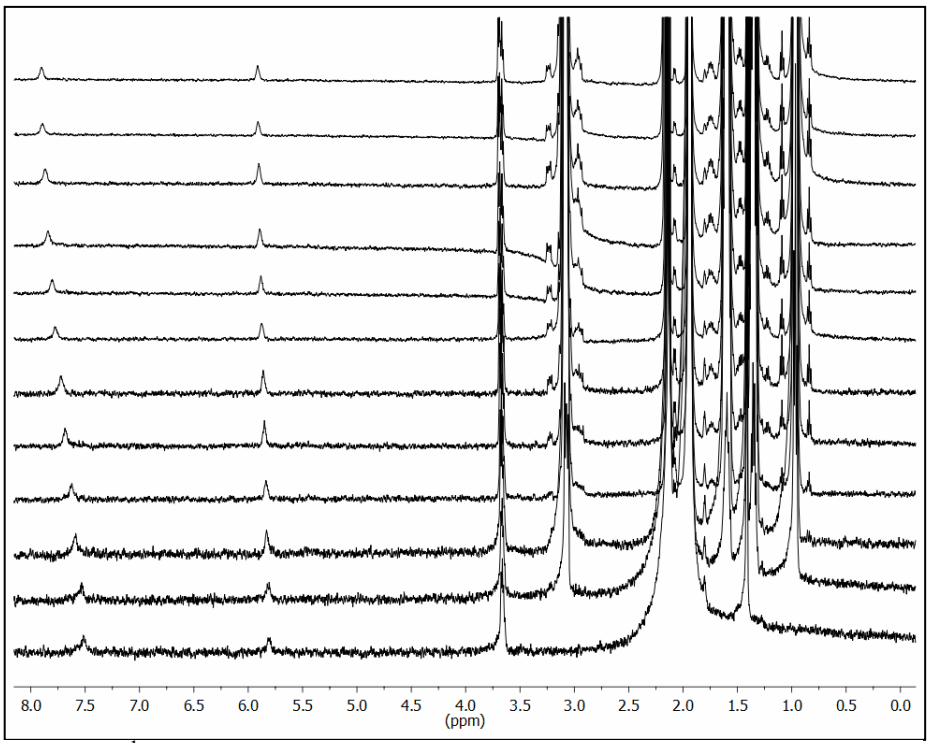

Fig. S31. ^{1}H NMR titration spectra of **2** with increasing amounts of TBA^{+} Br^{-} in MeCN-d_3(bottom to top).

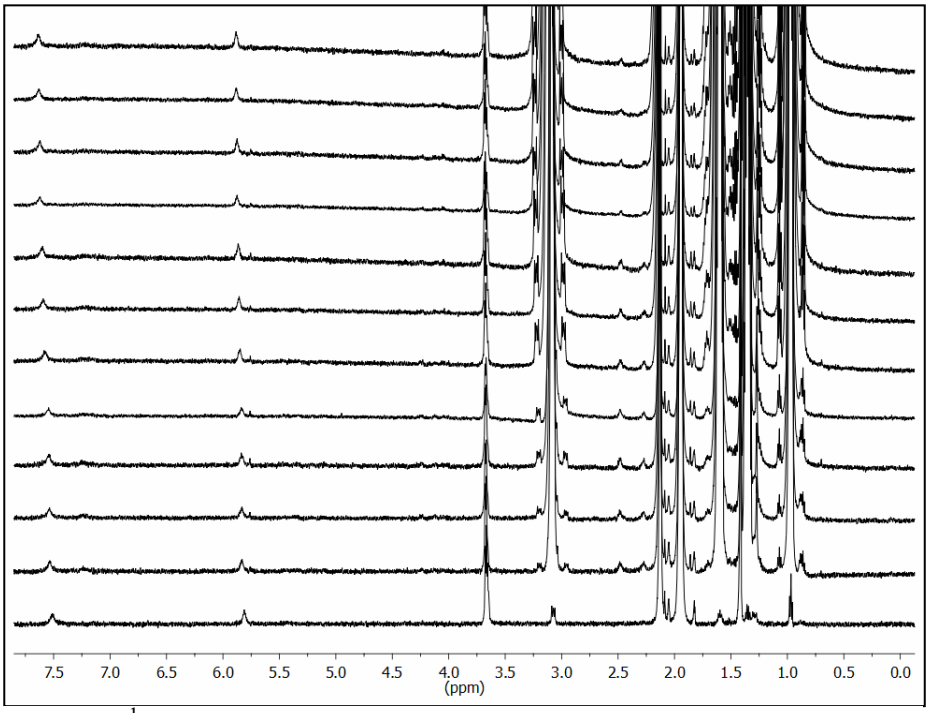

Fig. S32. ^{1}H NMR titration spectra of **2** with increasing amounts of $TBA^{+}\ I^{-}$ in MeCN-d_3(bottom to top).

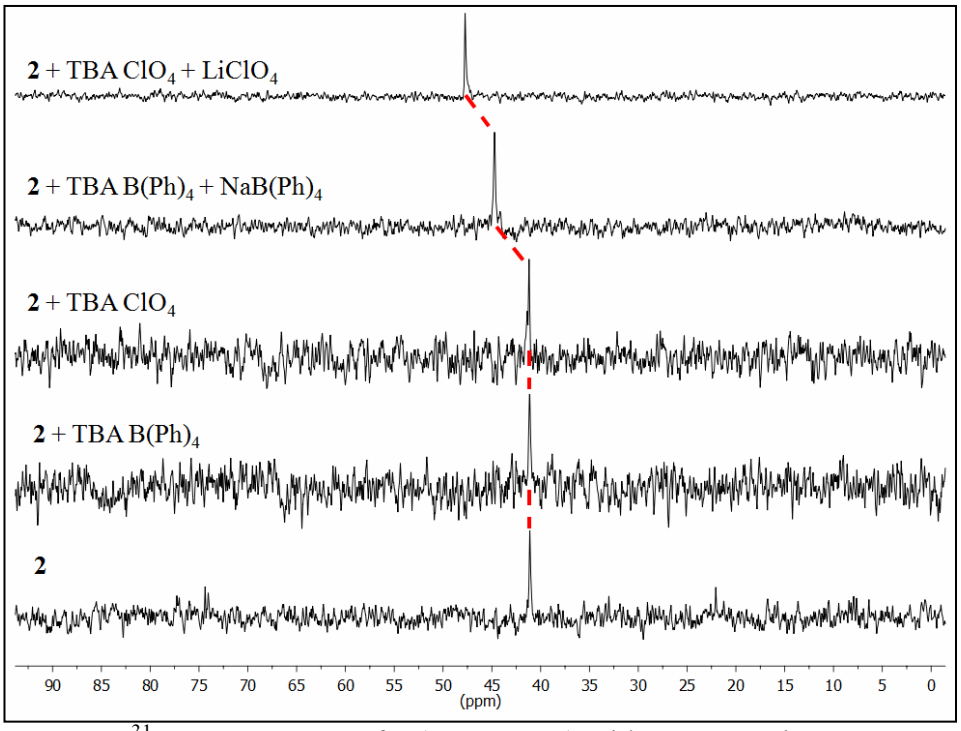

Fig. S33. ^{31}P NMR spectra of **2** (0.00128 M) with ca. 30 equiv. TBA $B(Ph)_4$, ca. 30 equiv. TBA ClO_4, ca. 30 equiv. TBA $B(Ph)_4$ + $NaB(Ph)_4$ and ca. 30 equiv. TBA ClO_4 + $LiClO_4$; MeCN-d_3.

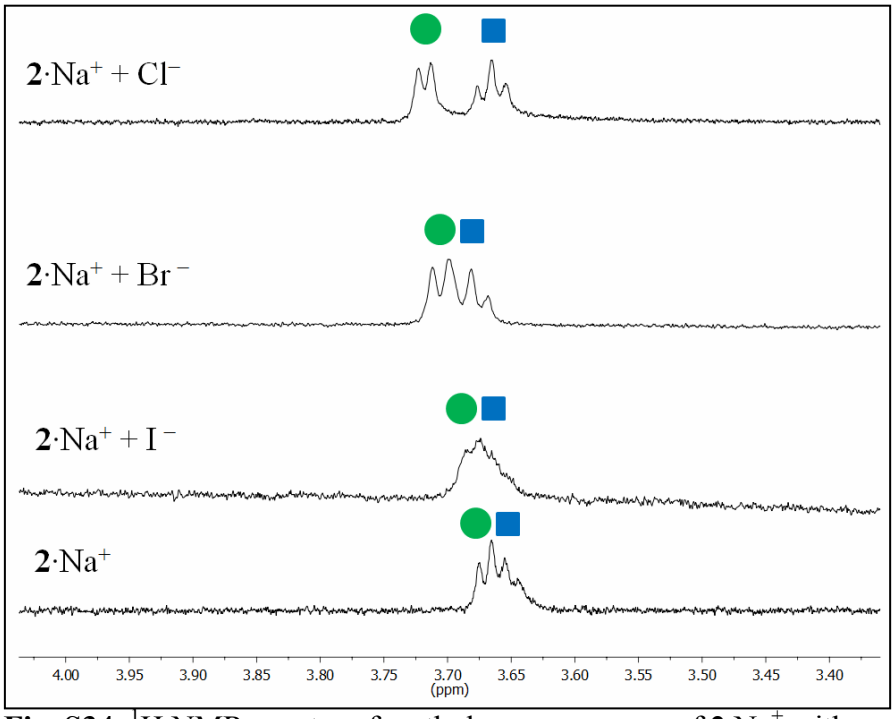

Fig. S34. ^{1}H NMR spectra of methylene resonances of **2**·Na^+ with excess iodide, bromide and chloride. Blue square = H_a. Green circle = H_b.

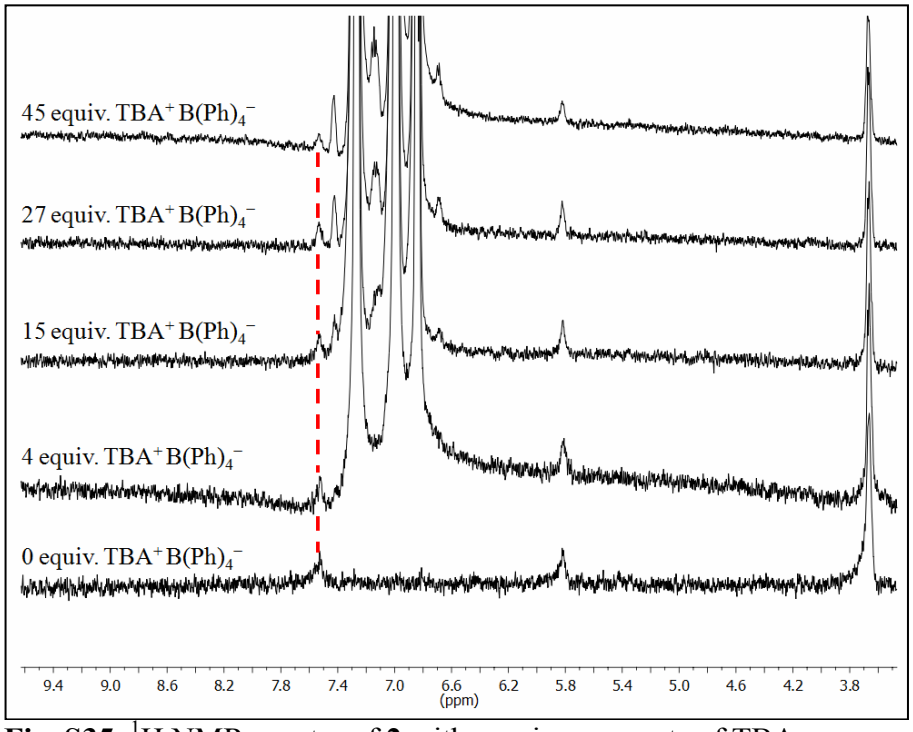

Fig. S35. ^{1}H NMR spectra of **2** with varying amounts of TBA tetraphenylborate.

5. X-Ray Crystal Structure Data for Receptors

5.1 Experimental Details

X-ray diffraction data were collected at 173 K on a Bruker Apex diffractometer using MoKα-radiation (λ=0.71073 Å). Absorption corrections were applied by SADABS.[6] In both cases crystals were very thin needles and as a result reflections at high angles were very weak. All structures were determined by direct methods and refined on F^2 by a full-matrix least-squares procedure. All non-H atoms were refined with anisotropic thermal parameters. H atoms at carbon atoms in both structures were refined in calculated positions in a rigid group model. H atoms at N atoms and in solvent water molecules involved in H-bonds were found on the residual density maps and refined with isotropic thermal parameters; the distances of 1.009 and 1.00 Å were used in the refinements as targets for N-H and O-H bond lengths, respectively. The Flack parameter for **3**·3 (DMSO) is 0.17(12). All calculations were performed by the Bruker SHELXTL 6.10 package.[7]

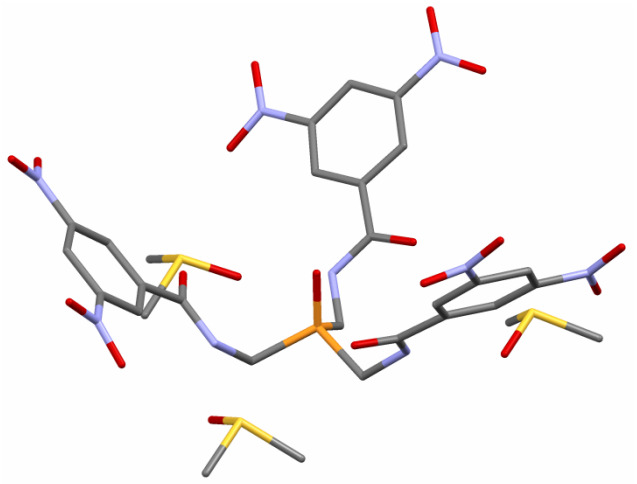

Fig. S36. X-Ray crystal structure of receptor **3** displaying endohedral phosphine oxide.

6. Optimized Geometry of 2·LiBr by ωB97X-D/6-311G*

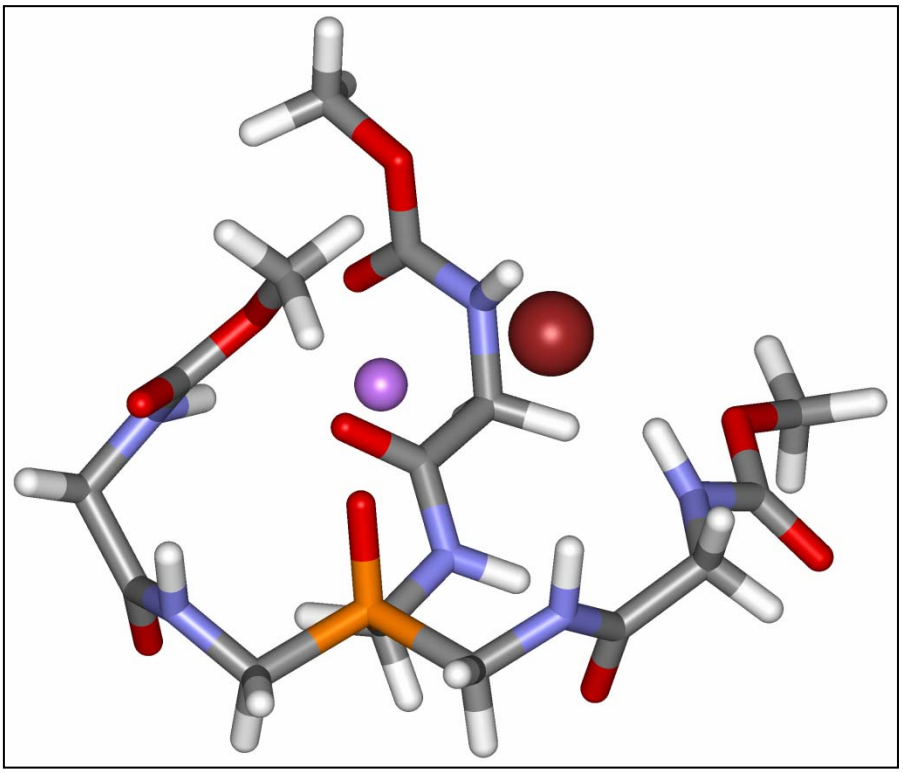

Fig. S37. DFT model of truncated **2**·LiBr showing endohedral phosphine oxide coordination.[8-10] Orange = P, red = O, blue = N, gray = C, white = H, purple = Li and burgundy = Br.

7. References

1. G. R. Fulmer, A. J. M. Miller, N. H. Sherden, H. E. Gottlieb, A. Nudelman, B. M. Stoltz, J. E. Bercaw and K. I. Goldberg, *Organometallics*, **29**, 2176-2179.
2. H. E. Gottlieb, V. Kotlyar and A. Nudelman, *J. Org. Chem.*, 1997, **62**, 7512-7515.
3. D. M. Rudkevich, G. Hilmersson and J. Rebek, *J. Am. Chem. Soc.*, 1998, **120**, 12216-12225.
4. For Job plots with lithium, an excess of lithium was present in both the host and guest solutions to maintain a constant concentration of lithium for all equilibria.
5. M. J. Hynes, *J. Chem. Soc., Dalton Trans.*, 1993, **2**, 311-312.
6. G. M. Sheldrick, Bruker/Siemens Area Detector Absorption Correction Program, Bruker AXS, Madison, WI, 1998.

7. SHELXTL-6.10 "Program for Structure Solution, Refinement and Presentation" BRUKER AXS Inc., 5465 East Cheryl Parkway, Madison, WI 53711-5373 USA
8. Y. Shao, L. F. Molnar, Y. Jung, J. Kussmann, C. Ochsenfeld, S. T. Brown, A. T. B. Gilbert, L. V. Slipchenko, S. V. Levchenko, D. P. O'Neill, R. A. DiStasio Jr, R. C. Lochan, T. Wang, G. J. O. Beran, N. A. Besley, J. M. Herbert, C. Yeh Lin, T. Van Voorhis, S. Hung Chien, A. Sodt, R. P. Steele, V. A. Rassolov, P. E. Maslen, P. P. Korambath, R. D. Adamson, B. Austin, J. Baker, E. F. C. Byrd, H. Dachsel, R. J. Doerksen, A. Dreuw, B. D. Dunietz, A. D. Dutoi, T. R. Furlani, S. R. Gwaltney, A. Heyden, S. Hirata, C.-P. Hsu, G. Kedziora, R. Z. Khalliulin, P. Klunzinger, A. M. Lee, M. S. Lee, W. Liang, I. Lotan, N. Nair, B. Peters, E. I. Proynov, P. A. Pieniazek, Y. Min Rhee, J. Ritchie, E. Rosta, C. David Sherrill, A. C. Simmonett, J. E. Subotnik, H. Lee Woodcock Iii, W. Zhang, A. T. Bell, A. K. Chakraborty, D. M. Chipman, F. J. Keil, A. Warshel, W. J. Hehre, H. F. Schaefer Iii, J. Kong, A. I. Krylov, P. M. W. Gill and M. Head-Gordon, *Phys. Chem. Chem. Phys.*, 2006, **8**, 3172-3191.
9. J.-D. Chai and M. Head-Gordon, *Phys. Chem. Chem. Phys.*, 2008, **10**, 6615-6620.
10. M. Swart, M. Sola and F. M. Bickelhaupt, *J. Chem. Phys.*, 2009, **131**, 94103-94112.